Estimating the size and abundance of dark matter subhaloes with gravitational millilensing

Héctor Vives-Arias[1], Jorge Jiménez-Vicente[2], Jose A. Muñoz[1], Evencio Mediavilla[3]

[1]Departamento de Astronomía y Astrofísica, Universidad de Valencia
[2]Departamento de Física Teórica y del Cosmos, Universidad de Granada
[3]Instituto de Astrofísica de Canarias

Abstract

We use 8 gravitational lens systems with quadruply imaged quasars and their observed flux ratio anomalies obtained using data in mid-infrared, radio or spectral narrow lines as a baseline, to estimate the amount of substructure in the dark matter halo of lens galaxies. We assume that the smooth gravitational potential of the galaxies is well modeled by a Singular Isothermal Ellipsoid (SIE) plus external shear (γ) and an additional Singular Isothermal Sphere (SIS) in some cases, and that the cause of the flux ratio anomalies is dark matter subhalos described by pseudo-Jaffe density profiles. Our Bayesian estimate for the Einstein radius of the subhalos is $b = 0.0003^{+0.0005}_{-0.0002}$ arcsec, and their abundance (as a fraction of the total surface density of the lens galaxy at the image positions) is $\alpha = 0.075^{+0.030}_{-0.021}$.

The missing satellites problem

Cold Dark Matter (CDM) numerical cosmological simulations predict that the dark matter haloes of galaxies contain hundreds or thousands of smaller satellites, or subhaloes, in stark contrast with the much lower number of luminous satellites observed around the Milky Way or other galaxies. This discrepancy could mean that such satellites do not exist and our models are wrong, or that they are there but some mechanism has depleted them of gas and stars or prevented them from accreting enough baryonic matter in the first place.

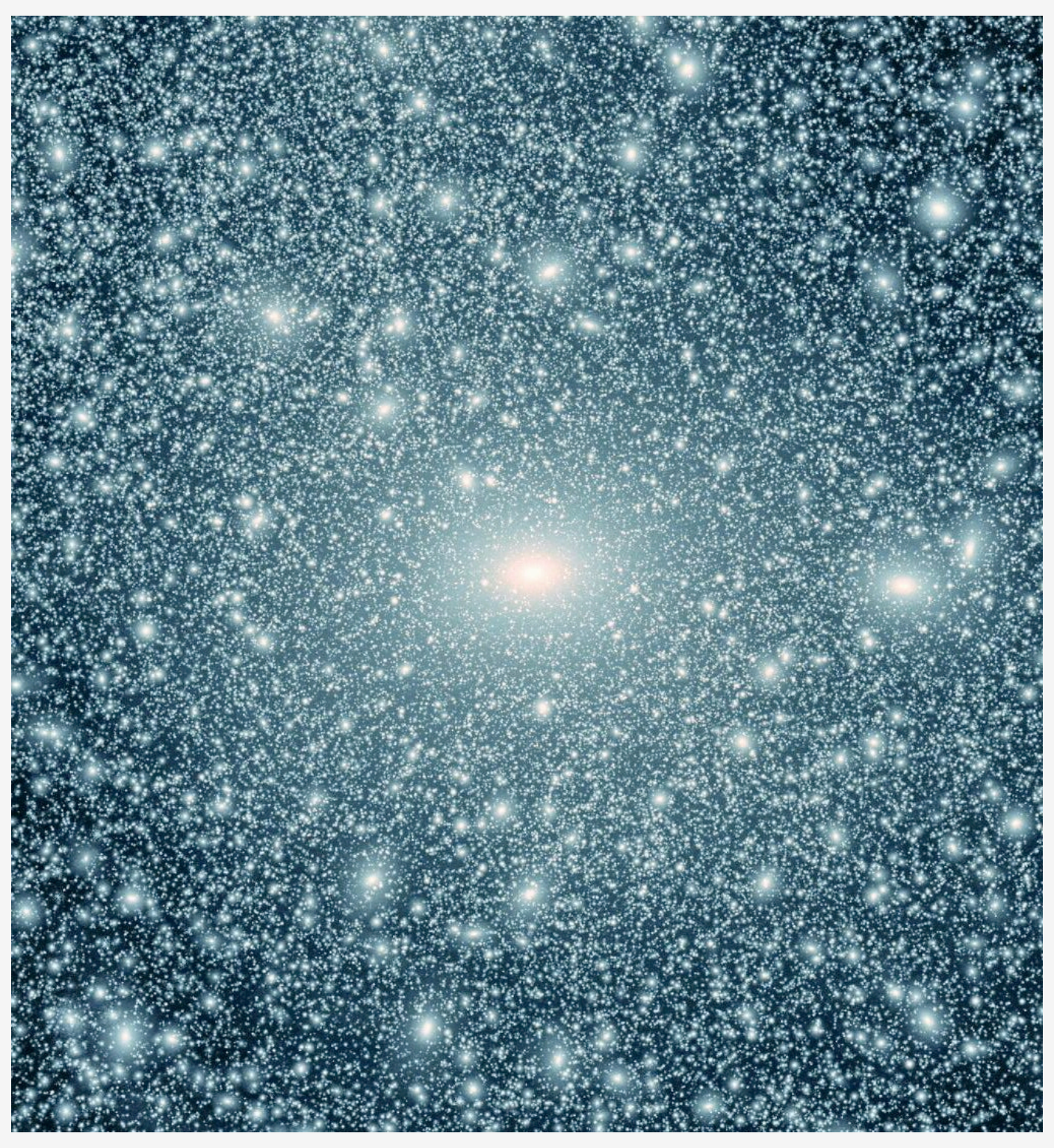

The dark matter distribution within the inner 200kpc of our Galactic halo. GHALO collaboration, Stadel, J. et al. (2008)

If these satellites do exist but are dark, one way of detecting them would be through gravitational lensing. There are systems in which a galaxy creates multiple images of a distant lensed quasar. The flux ratios between these images depend on the mass distribution of the lens, and sometimes there are anomalies in the observed fluxes with respect to what smooth models of the lens galaxy with no subhaloes would predict. Differential magnification caused by dark matter subhaloes (millilensing) could be the culprit.

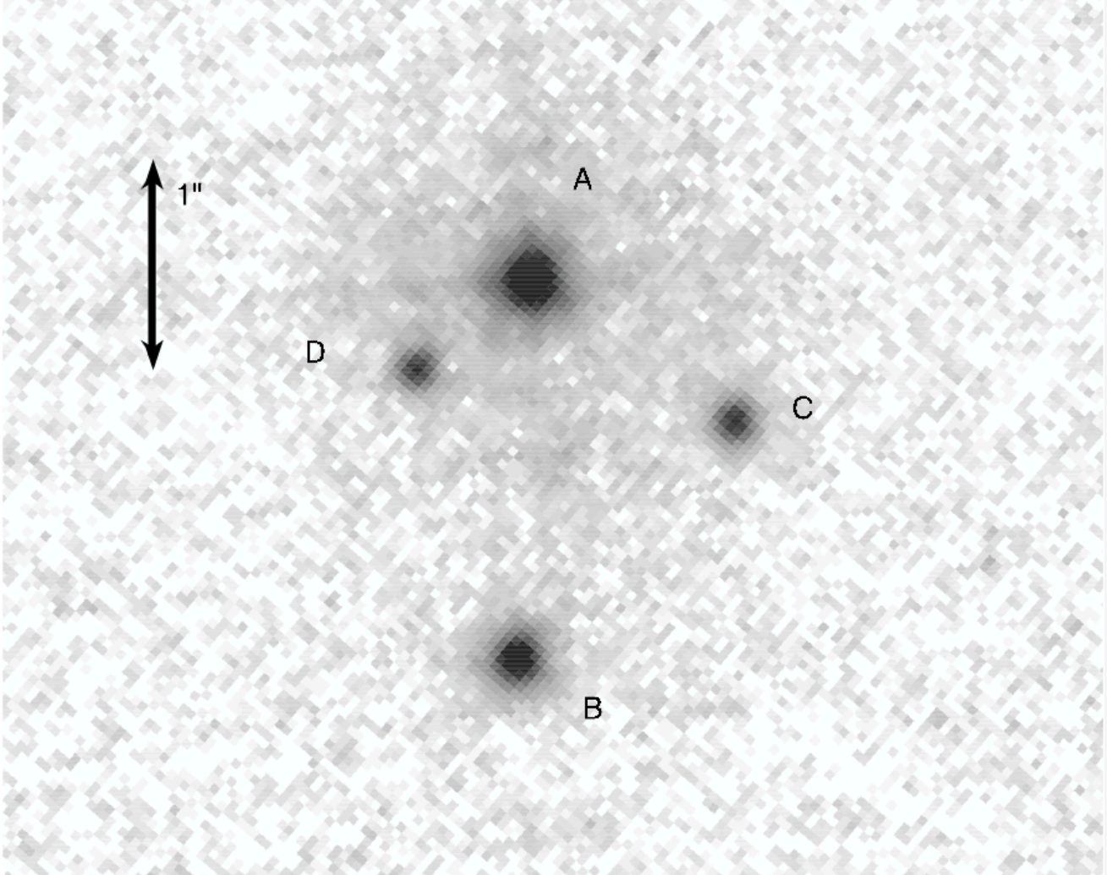

HST/WFC3 UV image of SDSS0924+0219, showing an anomalous flux ratio between images A and D.

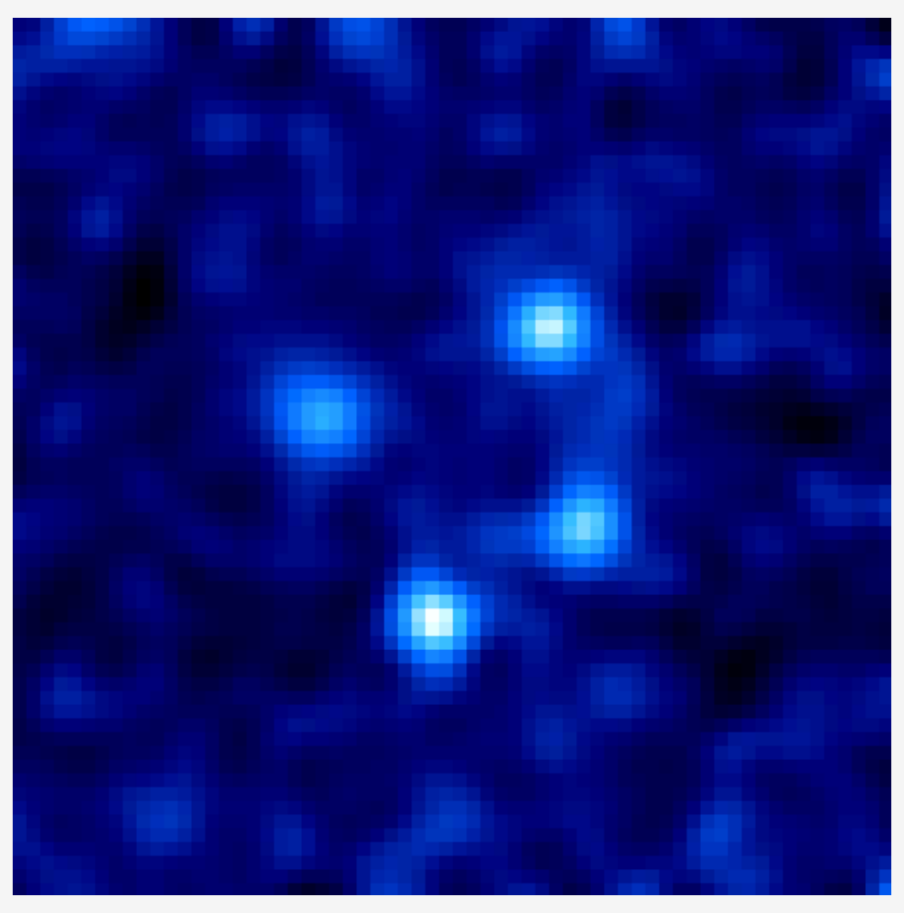

Mid-IR observation of the lensed system Q2237+0305. Vives-Arias, H. et al. (2016, arXiv:1606.03582)

Observational sample

The flux ratios of the quasar images can also be changed by differential extinction or microlensing from stars in the lens galaxy, so we are interested in observing light that is relatively immune to these effects. Microlensing magnification is stronger the smaller the source is, so we want light not from the continuum emitted by the accretion disk but from larger regions of the AGN like the dusty torus, the jet, or the narrow line region. These emit in the mid-infrared, radio, and narrow optical and near-infrared spectral lines, respectively, which makes it easy to obtain their flux ratios, and they are unaffected (or can be corrected) by extinction.

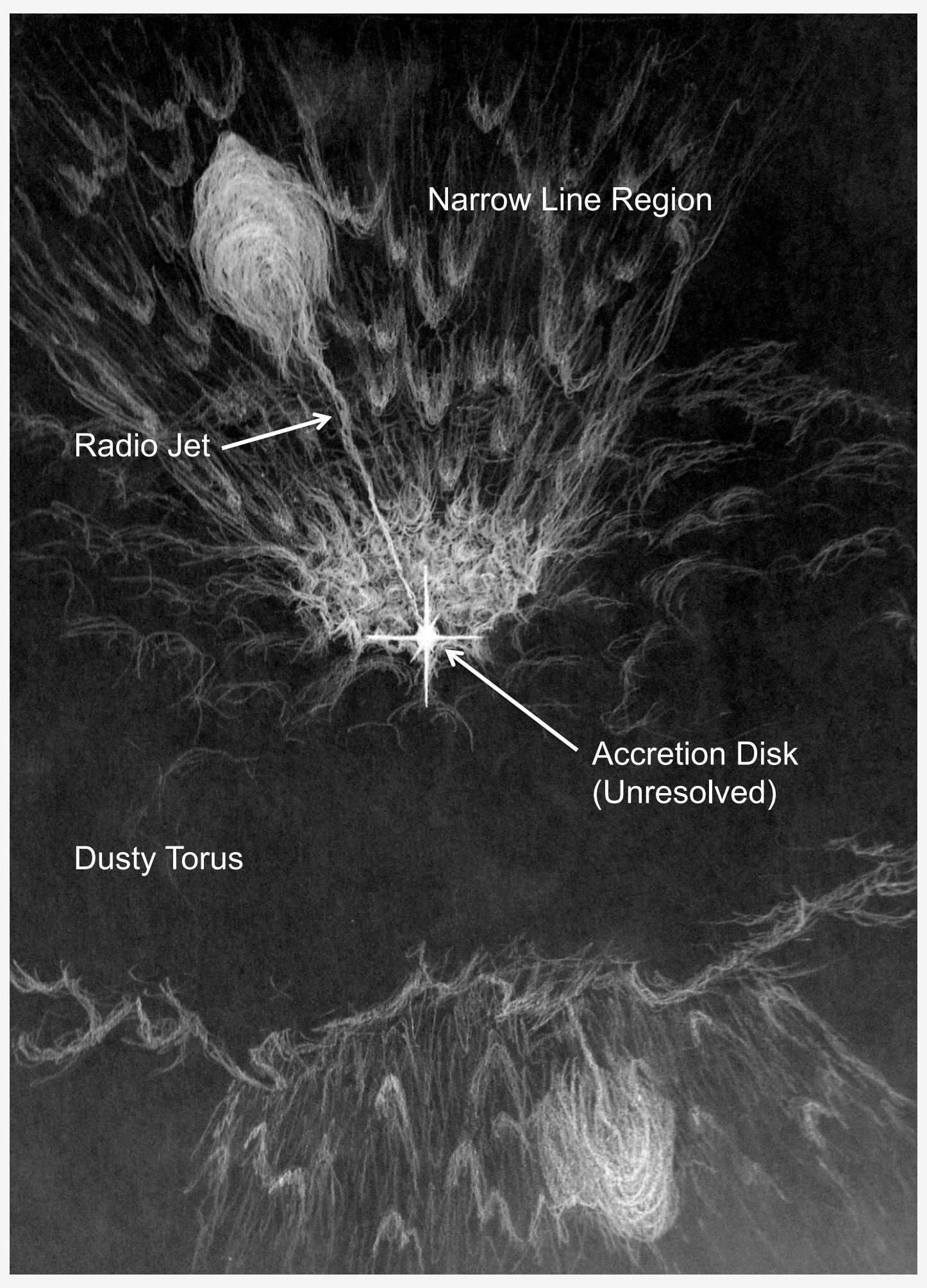

Artistic representation of an Active Galactic Nucleus (AGN) and its largest components.

Table 1. Predicted and observed flux ratios, and flux anomalies

Object	Model (constraints)	Ratios	Model	Line	IR	Radio	Δm_{lin}	Δm_{IR}	Δm_{radio}
B 0128+437[0,3]	SIE + γ $(\vec{x}_i, \vec{x}_{G1})$	B/A	0.72	—	—	0.58	—	—	0.23
		C/A	0.40	—	—	0.52	—	—	-0.28
		D/A	0.48	—	—	0.51	—	—	-0.07
MG 0414+0534[1,4]	SIE + γ + SIS $(\vec{x}_i, \vec{x}_{G1}, \vec{x}_{GX})$	A2/A1	1.03	—	0.90	0.90	—	0.14	0.14
		B/A1	0.29	—	0.36	0.37	—	-0.25	-0.28
		C/A1	0.15	—	0.12	0.15	—	0.22	0.00
HE 0435-1223[1,5]	SIE + γ $(\vec{x}_i, \vec{x}_{G1})$	A/C	0.94	1.41	—	1.05	-0.44	—	-0.12
		B/C	1.02	1.08	—	0.77	-0.06	—	0.31
		D/C	0.61	0.79	—	0.47	-0.28	—	0.28
B 0712+472[2,3]	SIE + γ $(\vec{x}_i, \vec{x}_{G1})$	B/A	1.08	—	—	0.84	—	—	0.27
		C/A	0.27	—	—	0.42	—	—	-0.48
		D/A	0.06	—	—	0.08	—	—	-0.36
PG 1115+080[1,6]	SIS + SIS $(\vec{x}_i, \vec{x}_{G1})$	A2/A1	0.95	1.00	0.93	—	-0.05	0.03	—
RXS J1131-1231[1,7]	SIE + γ $(\vec{x}_i, \vec{x}_{G1})$	A/B	1.62	1.97	—	—	-0.21	—	—
		C/B	0.94	1.33	—	—	-0.38	—	—
B J1422+231[1,3,8]	SIE + γ $(\vec{x}_i, \vec{x}_{G1})$	B/A	1.18	1.11	0.85	1.06	0.07	0.36	0.11
		C/A	0.62	0.54	0.57	0.55	0.15	0.09	0.13
		D/A	0.05	0.03	—	0.02	0.54	—	0.49
Q 2237+0305[9]	SIE $(\vec{x}_i, \vec{x}_{G1})$	B/A	0.89	—	0.97	—	—	-0.09	—
		C/A	0.45	—	0.51	—	—	-0.13	—
		D/A	0.82	—	0.92	—	—	-0.13	—

[0] Model ratios from Sluse et al. (2012, A&A, 538, A99).

[1] Model ratios from Schechter et al. (2014, ApJ, 793, 96).

[2] Model ratios from Xu et al. (2015, MNRAS, 447, 3189).

[3] Radio flux ratios from Koopmans et al. (2003, ApJ, 595, 712).

[4] Mid-IR flux ratios from Minezaki et al. (2009, ApJ , 697, 610), radio flux ratios from Rumbaugh et al. (2015, MNRAS, 450, 1042).

[5] Emission line flux ratios from Table 3 of Wisotzki et al. (2003, A&A, 408, 455), radio flux ratios from Jackson et al. (2015, MNRAS, 454, 287).

[6] Optical emission line flux ratios from Popović & Chartas (2005, MNRAS, 357, 135). Mid-IR data from Chiba et al. (2005, ApJ , 627, 53).

[7] [OIII] emission line flux ratios from Sluse et al. (2007, A&A, 468, 885).

[8] Optical emission line flux ratios from Impey et al. (1996, ApJ, 462, L53). Mid-IR data from Chiba et al. (2005, ApJ , 627, 53).

[9] Mid-IR and model flux ratios from Vives-Arias et al. (2016, arXiv:1606.03582).

In order to have well constrained models that predict the flux ratios without using the observed ones as constraints, we need quadruply lensed quasars. We selected systems from the literature that had been observed in radio, mid-IR, and spectral lines, and had been fit to smooth models using only Singular Isothermal Ellipsoids (SIE) plus an external shear (γ) and an additional Singular Isothermal Sphere (SIS) if needed.

Methods

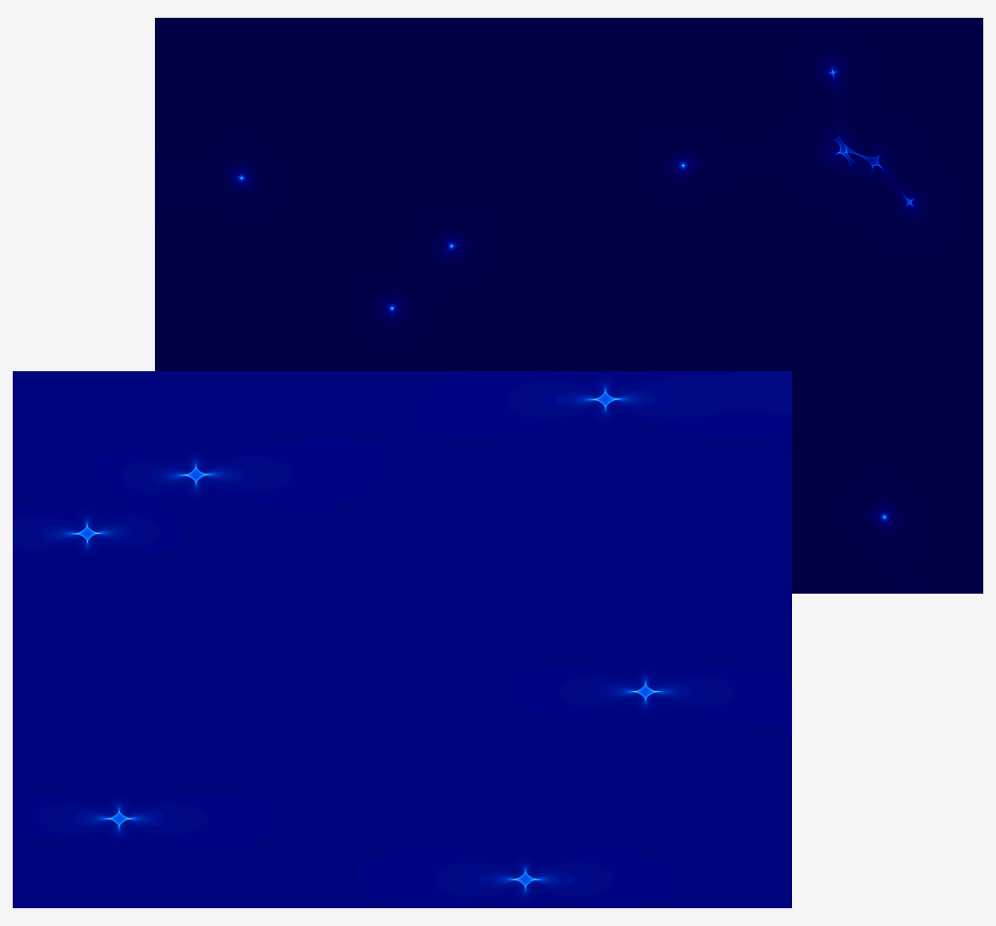

Magnification maps created by our subhaloes

We generated magnification maps for each quasar image and a range of Einstein radii (b, in arcseconds) and abundance of subhaloes (α, the fraction of the total surface density of the lens galaxy at the image positions), and modelled the subhaloes themselves with pseudo-Jaffe density profiles of equal mass in each case. These maps were used in a Bayesian analysis to estimate the probability of producing the observed anomalies in the flux ratios for each b and α, and therefore obtain probability density functions (PDFs) for each system. The mass range of the subhaloes is roughly 2×10^5 to 3×10^8 solar masses.

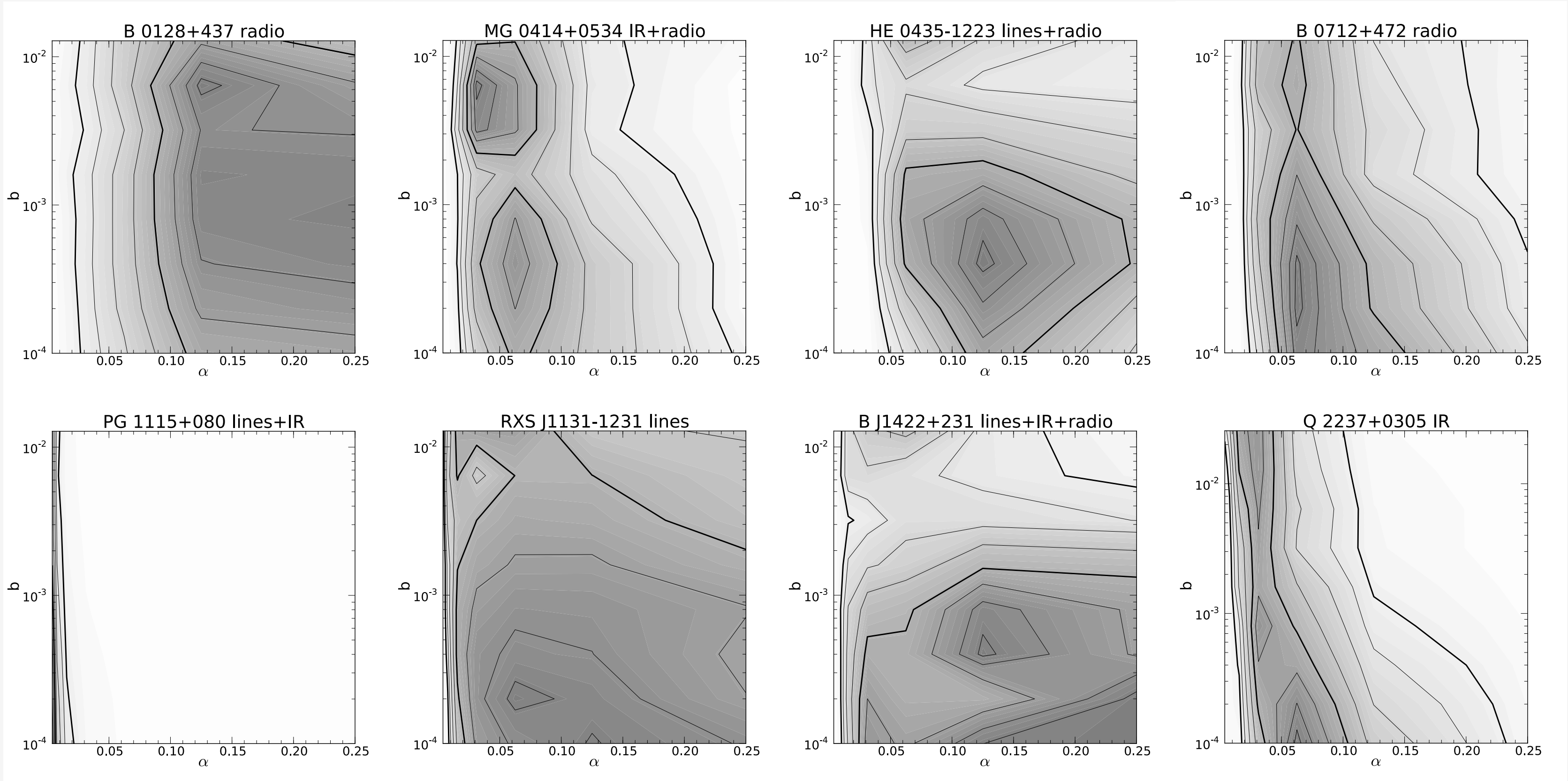

Results

When combining the PDFs of the 8 systems we studied, we obtain the following Bayesian estimates for the average Einstein radius b and abundance α of dark matter subhaloes in galaxies:

$$b = 0.0003^{+0.0005}_{-0.0002}$$

$$\alpha = 0.075^{+0.030}_{-0.021}$$

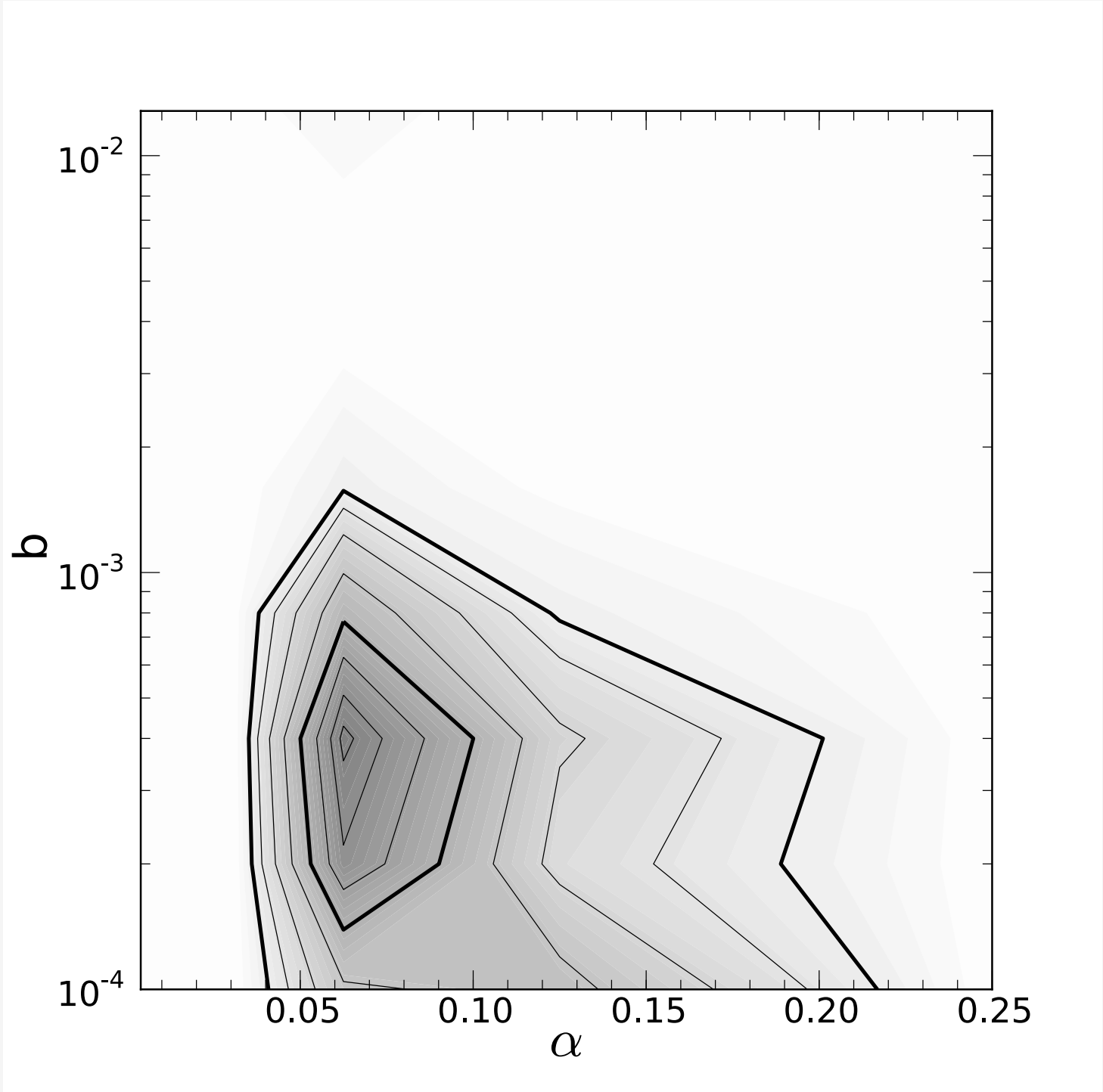

The expected value of the Einstein radius that we estimate corresponds to a subhalo mass of ~10^6 $M_\odot$. The abundance α is higher than the predictions of CDM simulations, but still marginally compatible at 2σ. It must be kept in mind that for this study we assumed that the galaxies are well modelled with SIE +γ(+SIS) profiles, and that the flux ratios are unaffected by systematics, extinction, microlensing or other perturbations. These are all factors that might lead to an overestimation of the anomalies, so the value obtained should probably be regarded as an upper limit only. Future work with more detailed mass models and a larger sample of systems will help constrain the actual values of the mass fraction that remains as satellites in the dark matter haloes of galaxies.